JOURNAL OF GEOPHYSICAL RESEARCH, VOL. 95, NO. B5, PAGES 6955–6966, MAY 10, 1990

Deconvolution of Mineral Absorption Bands: An Improved Approach

JESSICA M. SUNSHINE, CARLE M. PIETERS, AND STEPHEN F. PRATT

Department of Geological Sciences, Brown University, Providence, Rhode Island

Although visible and near-infrared reflectance spectra contain absorption bands that are characteristic of the composition and structure of the absorbing species, deconvolving a complex spectrum is nontrivial. An improved approach to spectral deconvolution is presented here that accurately represents absorption bands as discrete mathematical distributions and resolves composite absorption features into individual absorptions bands. The frequently used Gaussian model of absorption bands is first evaluated and shown to be inappropriate for the Fe^{2+} electronic transition absorptions in pyroxene spectra. Subsequently, a modified Gaussian model is derived using a power law relationship of energy to average bond length. This modified Gaussian model successfully depicts the characteristic 0.9-μm absorption feature in orthopyroxene spectra using a single distribution. The modified Gaussian model is also shown to provide an objective and consistent tool for deconvolving individual absorption bands in the more complex orthopyroxene, clinopyroxene, pyroxene mixtures, and olivine spectra. The ability of this new modified Gaussian model to describe the Fe^{2+} electronic transition absorption bands in both pyroxene and olivine spectra strongly suggests that it be the method of choice for analyzing all electronic transition bands.

INTRODUCTION

At visible and near-infrared wavelengths, reflectance spectra of minerals contain absorption features that are characteristic of the composition and crystal structure of the absorbing species [e.g., *Burns*, 1970*a*; *Marfunin*, 1979; *Adams*, 1974, 1975; *Hunt and Salisbury*, 1970]. As such, it is possible to use remotely sensed reflectance spectra as a basis for estimating the mineralogy of both terrestrial and extra-terrestrial surfaces [e.g., *McCord et al.*, 1988]. Recent advances in technology have resulted in the development of imaging spectrometers which allow the remote collection of reflectance data at high spectral and spatial resolution over a broad spectral range. Current and future exploration programs call for an increased use of imaging spectrometers from telescopic, airborne, and orbiting platforms to determine the mineralogy of various terrestrial and extra-terrestrial targets. The large influx of spectral reflectance measurements from such missions requires a consistent approach to the classification of absorption features.

In order to characterize absorption features, it is necessary to understand the physics that control the absorption process. However, absorptions in geologic surfaces containing intimately mixed mineralogies are complex and only partially understood. Electromagnetic energy interacts with a particulate interface through a combination of first surface (or specular) reflection transmission, absorption, diffraction, and multiple scattering from adjacent particles [e.g., *Wendlandt and Hecht*, 1966; *Körtum*, 1969]. Although reflectance spectra at visible and near-infrared wavelengths contain diagnostic information, deconvolving the composite spectral signals of multi-component target surfaces to reveal individual components and their modal mineralogy is nontrivial.

Paper number 89JB03621.
0148-0227/90/89JB-03621$05.00

A variety of theoretical and empirical approaches have been developed to address this problem. The use of Hapke's theoretical radiative transfer model to the extraction of modal abundance from reflectance spectra of geologic materials [*Hapke*, 1981; *Clark and Roush*, 1984] has been tested in the laboratory [e.g., *Johnson et al.*, 1983; *Clark*, 1987; *Nelson and Clark*, 1988; *Mustard and Pieters*, 1989] and the field [e.g., *Mustard and Pieters*, 1987] and has been shown to be able to deconvolve mixture spectra to within an accuracy of approximately 5%. This method requires detailed knowledge of the spectral reflectance properties of the end-member components in mixture spectra and is thus most successful for applications that allow representative samples to be obtained. The practical applicability of the Hapke model to regions where ground truth is unavailable can be greatly enhanced if it is utilized in conjunction with other methods that can determine probable mineralogic end-members.

Empirical approaches to the extraction of mineralogical information from the absorption features in reflectance spectra have also been undertaken. A variety of successful schemes have been developed that quantify observed trends in albedo and/or absorption characteristics for specific minerals in carefully prepared laboratory mixtures [e.g., *Clark*, 1981; *Cloutis et al.*, 1986; *Gaffey*, 1986]. While these empirical studies are useful as diagnostic tools for mixtures of specific minerals, they are limited to applications that only involve the minerals studied.

A more general method of spectral deconvolution is presented here, which resolves spectra into individual absorption bands by representing these absorption bands with discrete mathematical distributions. Use of this quantitative deconvolution method for a spectrum of an unknown material is dependent only the spectrum itself. It thus provides an objective and consistent tool for examining the individual absorption bands in spectra. Interpretation of the resultant absorption bands can then be made based on independent empirical and/or theoretical studies.

Spectra of pure mineral separates of olivine, pyroxene, and mixtures of pyroxenes were obtained in order to test

these deconvolution methods. The Gaussian model of absorption bands is discussed and evaluated in detail in the following sections. Although it has commonly been invoked, the Gaussian model proves to be an inadequate description of the electronic transition absorptions found in pyroxene spectra. Subsequently, a modified Gaussian model is derived and shown to successfully model the electronic transition absorptions in pyroxene, pyroxene mixtures, and olivine spectra. Preliminary results from this study were presented by *Sunshine et al.* [1988, 1989].

Gaussian Model of Absorption Bands and Its Assumptions

The underlying assumption of the Gaussian model is that absorption features observed in visible and near-infrared spectra are composed of absorption bands which are inherently Gaussian in shape. If this is true, spectral features can be resolved into absorption bands by fitting them with Gaussian distributions. Since Gaussian deconvolution has produced results that often correlate with specific real absorptions without requiring more complex functions, this method has been used by several investigators as a quantitative tool in spectral studies [*Burns*, 1970*b*; *Smith and Strens*, 1976; *Farr et al.*, 1980; *McCord et al.*, 1981; *Clark*, 1981; *Singer*, 1981; *Clark and Roush*, 1984; *Huguenin and Jones*, 1986; *Gaffey*, 1986; *Roush and Singer*, 1986]. As pointed out by *Roush and Singer* [1986], at the very least a Gaussian deconvolution should produce a unique fit for a given mineral (under certain reasonable restraints) and thus, even if not physically realistic, could provide a useful aid in the analysis and classification of absorption features.

Under the central limit theorem of statistics, a Gaussian, or normal distribution, can be used to represent all random distributions given a large enough sample population. A Gaussian distribution in a random variable x, $g(x)$, is expressed in terms of its center (mean) μ, width (standard deviation) σ, and strength (amplitude) s:

$$g(x) = s \cdot \exp\left\{\frac{-(x-\mu)^2}{2\sigma^2}\right\} \quad (1)$$

In order to apply the central limit theorem to spectra, the various electronic and vibrational processes that cause absorption bands must each be randomly distributed in a random variable x and result from a statistically significant number of events. There are a sufficient number of photons in incident electromagnetic radiation to satisfy the assumption of a large sample population. Randomness, however, is more difficult to justify but has been assumed to occur due to the effects of thermal vibrations and/or minor variations in crystal structures. On the basis of the examination of absorption bands in transmission spectra, it has commonly been assumed that absorption bands are distributed around discrete energies [e.g., *Farr et al.*, 1980; *McCord et al.*, 1981]. If each of these assumptions hold, the probability of an absorption can be considered to be randomly distributed in energy and an absorption band can be modeled with a Gaussian distribution (equation (1)), where the random variable x is energy.

In transmission spectra, absorption bands not only occur around discrete energies but also obey the Beer-Lambert law:

$$I = I_0 \exp(-\alpha d) \quad (2)$$

where α is the absorption coefficient and d is the optical path length. At visible and near-infrared wavelengths, absorption bands in reflectance spectra are expected to behave similarly because the absorptions primarily occur as radiation is transmitted through the solid particles. In order to represent mathematically the reflectance spectra as linear combinations of absorption bands that occur around discrete energies, it is necessary to carry out the Gaussian model of absorption bands in natural log reflectance and energy.

In addition, observations of natural surfaces indicate that absorption features in many reflectance spectra are superimposed onto a base curve or "continuum" [e.g., *McCord et al.*, 1981]. The physical causes of the continuum are poorly understood. Often it is considered to represent a combination of phenomena including first surface reflectance, multiple scattering, wings of strong ultraviolet absorptions, or absorptions from materials with constant spectral signatures [e.g., *Burns*, 1970*a*; *Gaffey*, 1976; *Pieters*, 1978; *Marfunin*, 1979; *Clark and Roush*, 1984; *Huguenin and Jones*, 1986; *Yon and Pieters*, 1988]. Although the causes of continua are difficult to determine, for consistency the continua used in these analyses are linear functions of energy. In general, any reflectance spectrum will contain several absorption features and as such, the Gaussian model of a spectrum consists of multiple distributions, superimposed onto a continuum.

Experimental Approach

Reflectance spectra of pyroxene and olivine were used to assess the validity of each deconvolution model. These minerals were selected for analysis due to their relative abundance among the rock-forming minerals of the solar system and their well described spectral character [*Burns*, 1970*a*, *b*; *Adams*, 1974, 1975; *Hazen et al.*, 1978; *Rossman*, 1980]. As seen in Figure 1, the spectrum of olivine is dominated by a complex absorption centered near 1.0 μm, while the pyroxene spectrum is dominated by its characteristic absorption features near 1.0 and 2.0 μm. In both cases, these absorptions are produced by spin-allowed electronic transitions of Fe^{2+} in distorted octahedral (M1 and M2) crystal field sites [*Burns*, 1970*a*]. Furthermore, the centers of the characteristic pyroxene absorption bands systematically vary with increasing iron and calcium concentration from 0.90 to 1.05 μm and 1.80 to 2.30 μm, respectively [*Adams*, 1974; *Hazen et al.*, 1978] and thus can be use to infer pyroxene composition.

The samples used in this initial study are an enstatite from Webster, North Carolina (Opx), a clinopyroxene from a Hawaiian volcanic bomb (Cpx), and an olivine from Hawaiian green beach sand (located near South Point). The compositions of these minerals are given in Table 1. Hand-picked mineral separates of these samples were crushed and wet-sieved with ethanol into 45-75 μm particle size separates. In addition, seven mass fraction mixtures of the two pyroxenes were created. Spectra of the olivine, the pyroxenes, and the pyroxene mass fraction mixtures were obtained from 0.325 to 2.600 μm at 5 nm sampling resolution using the RELAB bidirectional spectrometer and are shown in Figures 1 and 2. The RELAB instrument is specifically designed to simulate, in the laboratory, the viewing geometries used in remote measurements [*Pieters*,

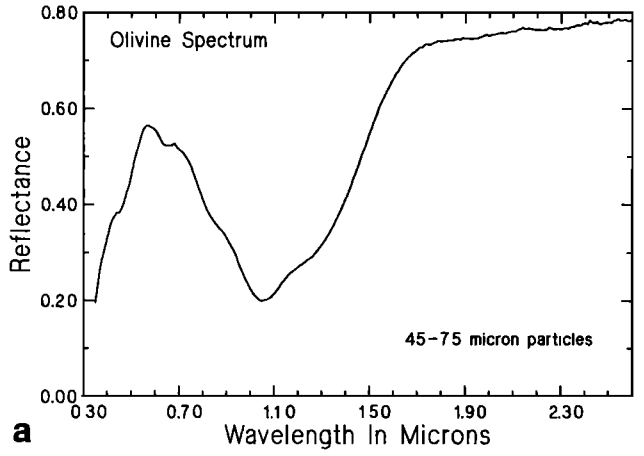

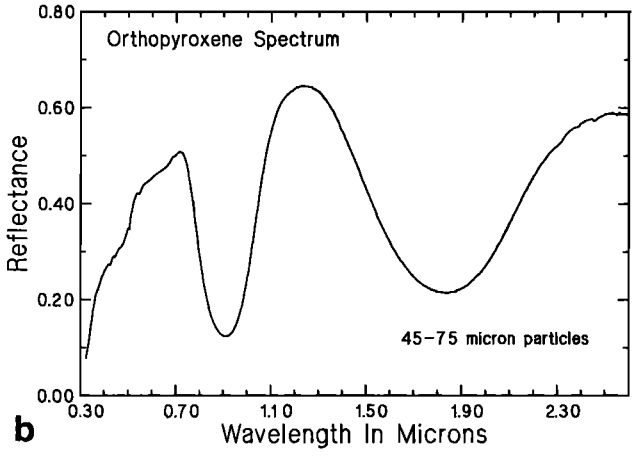

Fig. 1. (*a*) The reflectance spectrum (45-75 μm particles) of the olivine used in this study. The olivine spectrum is dominated by a multiple absorption feature centered near 1.0 μm. (*b*) The reflectance spectrum (45-75 μm particles) of the orthopyroxene used in this study. The pyroxene spectrum is dominated by the characteristic absorption features centered near 1.0 and 2.0 μm.

TABLE 1. Chemical Analysis of Minerals Used in This Study

	Clinopyroxene PP-CMP-21	Orthopyroxene PE-CMP-30	Olivine[a] PO-CMP-25
SiO_2	49.69	56.23	38.90
TiO_2	0.79	0.02	0.03
Al_2O_3	6.40	1.02	0.46
Fe_2O_3	(as FeO)	(as FeO)	(as FeO)
FeO	6.29	8.53	10.7
MgO	15.14	32.81	47.20
CaO	20.92	0.41	0.41
Na_2O	0.40	0.01	0.00
K_2O	0.01	0.00	0.02
MnO	0.12	0.19	0.22
Total	99.76	99.22	98.71
	$Wo_{45.59}$ $En_{45.89}$ $Fs_{8.52}$	$Wo_{0.78}$ $En_{87.03}$ $Fs_{12.19}$	Fo_{89}

[a] From Singer [1981].

1983]. A 30° incident angle and a 0° emission angle (measured from the vertical) were chosen for these measurements.

Analysis of these spectra was made possible by the development of an enhanced Gaussian fitting package. This relatively fast routine, based on the nonlinear least squares algorithm developed by *Kaper et al.* [1966] permits the simultaneous analysis of an entire spectrum. From initial estimates provided by the investigator, the fitting procedure iteratively adjusts the model parameters (Gaussian widths, strengths, and centers, as well as continuum slope and intercept) until a negligible improvement in the overall fit is obtained. Additional Gaussian distributions can be added as deemed necessary based on an examination of the residual error between the measured and the modeled spectra. The mathematics of this procedure, as it specifically applies to reflectance spectra, are presented in detail in the appendix.

A fit is considered complete when the residual error, defined as the root mean square (RMS) error of the difference between the model and the actual data (see the appendix, equation (A14)), is of the same order of magnitude as the observational uncertainties. The observational errors in the laboratory spectra used here are approximately 0.25%. As such, the fitting routine is terminated when the RMS error of

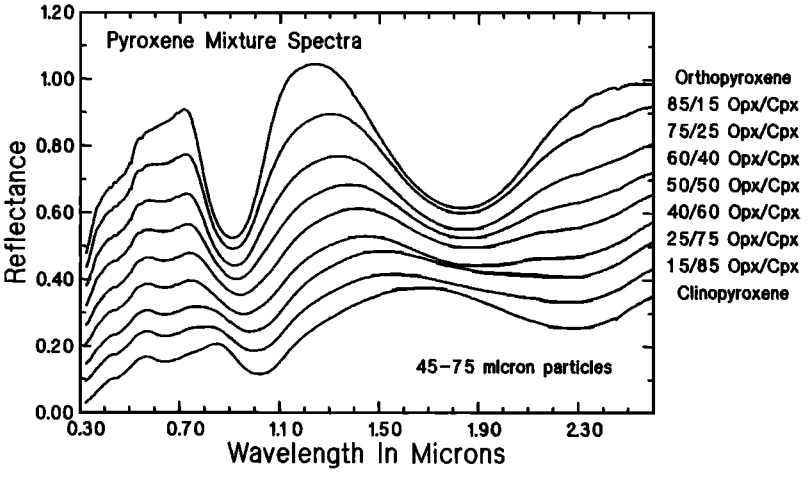

Fig. 2. The reflectance spectra (45-75 μm particles) of the pyroxene mass fraction mixtures. They are displayed from bottom to top with increasing orthopyroxene fraction and a 5% offset in reflectance between each successive spectrum.

the residual is of order of magnitude of tenths of a percent, or more likely, when the improvement of the RMS residual error in several successive iterations is negligible (of magnitude 10^{-5} or less).

Inadequacies of the Gaussian Model for Electronic Transition Absorption Bands

One goal of the investigation reported here is to determine if Gaussian deconvolutions accurately represent physical phenomenon and to examine whether Gaussian analysis provides a consistent and unique method for the extraction of compositional information from reflectance spectra.

The complexity of the Fe^{2+} absorption features found in olivine spectra make them natural candidates for Gaussian analysis. An olivine spectrum, the continuum, the Gaussian distributions that comprise its fit, and the residual error of that fit are shown in Figure 3*a*. Although the analysis is carried out in natural log reflectance and energy, because reflectance spectra are often displayed as a function of wavelength, all subsequent data will be shown in natural log reflectance and wavelength. This causes the continuum that is a linear function of energy to appear curved (Figure 3*b*). Gaussian analysis of an olivine reflectance spectrum reveals that the 1.0-μm absorption feature can be represented by three Gaussian distributions [*Singer*, 1981]. This result is expected from transmission studies that indicate that the 1.0-μm olivine feature arises due to three independent absorption bands [*Burns*, 1970*b*]. Unfortunately, olivine does not provide a good test of the model because it requires three distributions, and thus nine free parameters, all within the 1.0-μm region. Given this much flexibility, almost any function could provide a reasonable fit regardless of whether or not it physically represents the three absorption bands that comprise the absorption feature.

A better test would be to model absorption features that

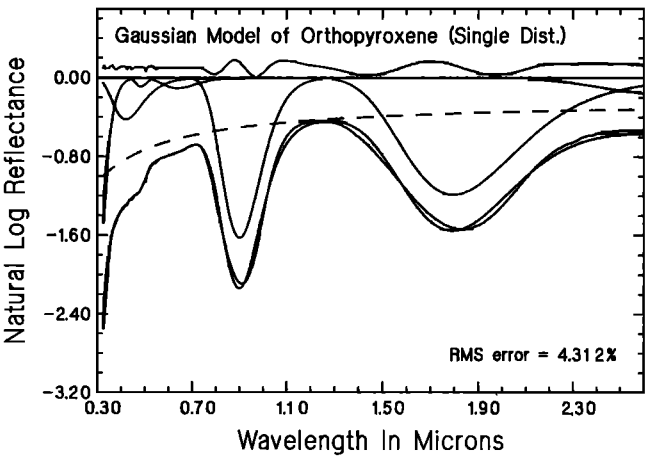

Fig. 4. The Gaussian model of the orthopyroxene reflectance spectrum (45-75 μm particles) using only single distributions for the absorption near 1.0 and 2.0 μm. This model produces a poor fit and an unacceptably high residual error.

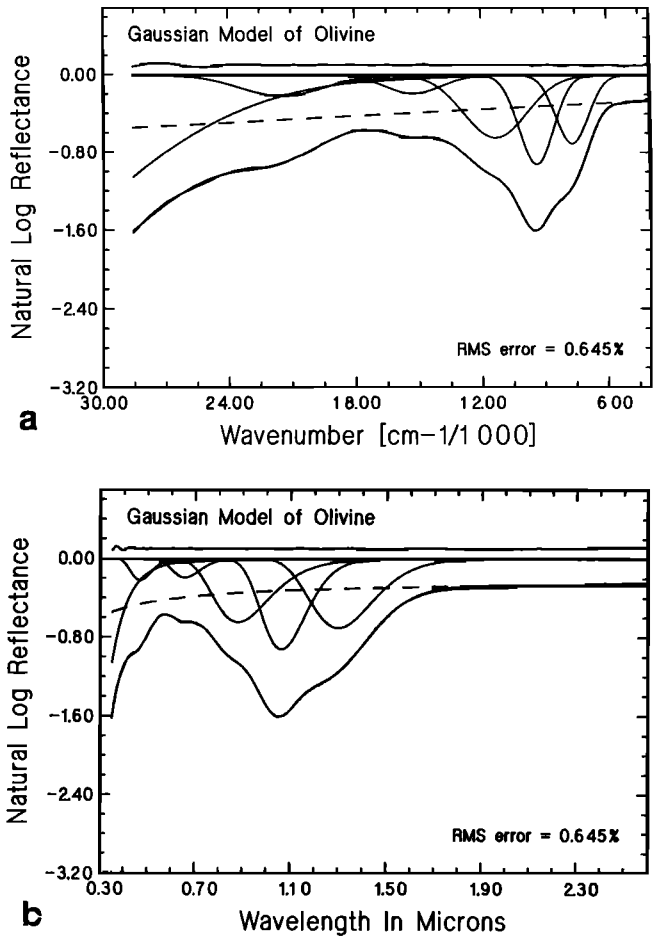

Fig. 3. (*a*) The Gaussian model of the olivine reflectance spectrum (45-75 μm particles). In this and all subsequent figures the model components are (from bottom to top): the modeled spectrum superimposed on to the reflectance spectrum, the continuum (dashed line) that is a linear function of energy (wave number), the individual Gaussian distributions that comprise the model and the residual error between the model and the actual spectra (offset 10% for clarity). (*b*) The Gaussian model of the olivine reflectance spectrum (45-75 μm particles). As in Fig. 3*a* but displayed as a function of wavelength. This causes the continuum that was a linear function of energy to appear curved.

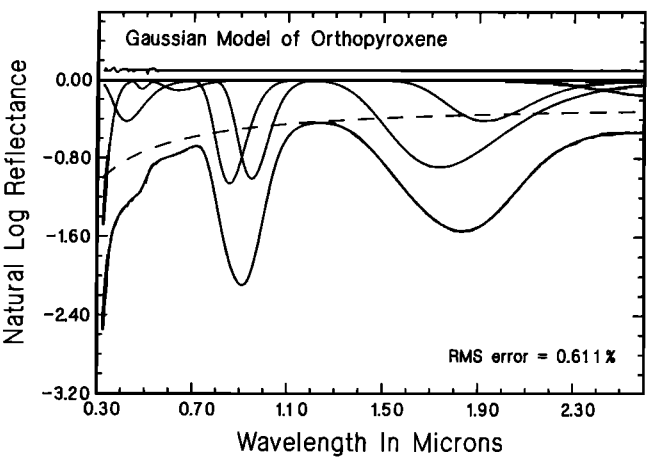

Fig. 5. The Gaussian model of the orthopyroxene reflectance spectrum (45-75 μm particles) using two Gaussian distributions for both of the absorption features near 1.0 and 2.0 μm. While this produces an acceptable fit to the features, it is contrary to expectations that these absorptions are each caused by primarily one electronic transition absorption band.

are believed to result from single absorption bands, such as the absorption features near 1.0 and 2.0 μm in the orthopyroxene spectrum. However, as shown in Figure 4, a Gaussian analysis of the orthopyroxene reflectance spectrum, using single distributions for each of the dominant absorptions produces an obviously poor fit with an RMS residual error of 4.32%. In order to reduce the residual error to the order of magnitude of the observational errors, it is necessary to use two Gaussian distributions for both of the absorption features near 1.0 and 2.0 μm (Figure 5). While this produces an acceptable fit to the features, it is contrary to our expectation that these absorptions are each caused primarily by one electronic transition absorption band.

These apparently spurious Gaussians, suggest that the Gaussian model may not reflect the actual physical processes of absorption. As suggested by *Singer* [1981], this may be a product of attempting to model an inherently asymmetric feature with symmetric Gaussian distributions. The Gaussian model may nonetheless provide a consistent tool for compositional analysis of spectra. In order to examine this potential, a Gaussian analysis of the spectra orthopyroxene, clinopyroxene and pyroxene mixtures was performed.

The Gaussian deconvolution of the orthopyroxene spectrum (Figure 5) consists of nine discrete Gaussian distributions, including two Gaussians in each of the dominant absorption features, superimposed onto a continuum. Similarly, the Gaussian deconvolution of the clinopyroxene spectrum, shown in Figure 6, also consists of a continuum and nine Gaussian distributions. Here again, the 1.0- and 2.0-μm absorption features required multiple Gaussians. The model fits to both of the pyroxenes produce RMS residual errors on the order of 0.5%.

On the basis of the Gaussian deconvolutions of these two pyroxene end-member spectra, each of the seven mass fraction pyroxene mixture spectra are modeled using Gaussian distributions with centers fixed at the wavelengths determined for the pure orthopyroxene and clinopyroxene end-members. Although each end-member spectrum consists of nine Gaussians, the first four distributions occur at very similar wavelengths for both end-members. These centers are too close to distinguish in the mixture spectra and as such, each mixture spectrum is modeled with 14 (rather than 18) Gaussians superimposed onto a continuum. A Gaussian analysis of the mixture spectra under these constraints yields RMS residual errors on the order of 0.5%. The constrained model fits to the 75/25 Opx/Cpx and 25/75 Opx/Cpx mixture spectra are shown in Figure 7, as examples.

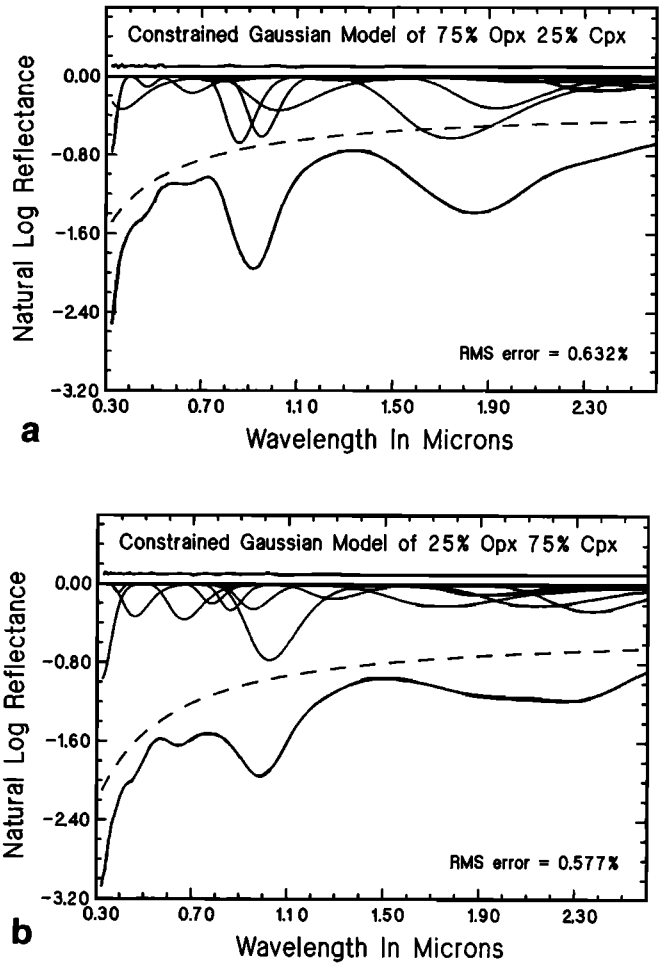

Fig. 7. (*a*) The Gaussian model of the 75% orthopyroxene 25% clinopyroxene mixture reflectance spectrum (45-75 μm particles). (*b*) The Gaussian model of the 25% orthopyroxene 75% clinopyroxene mixture reflectance spectrum (45-75 μm particles). These models are constrained to have the Gaussian distributions with centers fixed at the wavelengths determined for the pyroxene end-member spectra. Under such constraints, these models of pyroxene mixture spectra reflect the proportion of clinopyroxene in each sample.

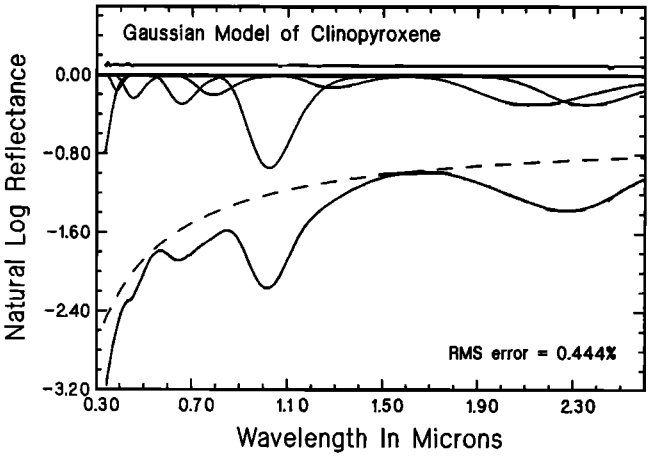

Fig. 6. The Gaussian model to the clinopyroxene reflectance spectrum (45-75 μm particles). Note that multiple Gaussian distributions are required for both of the absorption features near 1.0 and 2.0 μm.

While this constrained Gaussian analysis produces acceptable fits, to truly be useful, Gaussian analysis must be able to extract accurate results from the spectra of pyroxene mixtures without predetermined knowledge of their spectral components. To assess the feasibility of this, the mixture spectra were modeled with the constraints on the Gaussian centers removed. For example, with 14 unconstrained Gaussians the resulting fit to the 75/25 Opx/Cpx spectrum, shown in Figure 8, is still excellent. However, the Gaussian parameters of this unconstrained model bear no resemblance to those of the known pyroxene end-member components. As such, the Gaussian analysis of mixture spectra does not reveal any useful compositional information.

The inability of the Gaussian model to accurately

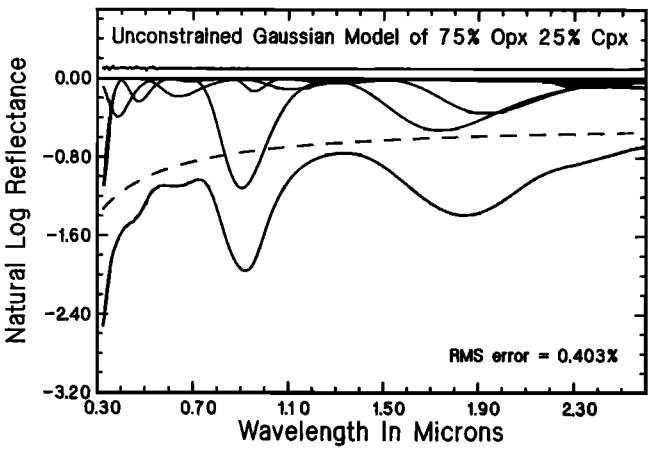

Fig. 8. The Gaussian model of the 75% orthopyroxene 25% clinopyroxene mixture reflectance spectrum (45-75 μm particles) with the constraints on the band centers removed. While this produces an acceptable fit, this Gaussian deconvolution bears no resemblance to the deconvolutions of the known pyroxene end-members.

characterize pyroxene mixture spectra is not surprising, since it requires multiple Gaussian distributions in order to accurately describe single electronic transition absorption bands. Using spurious Gaussian distributions to model the pyroxene end-member spectra results in 44 free parameters (14 Gaussian distributions each with three free parameters and a continuum with two) for each pyroxene mixture spectrum. This over-abundance of parameters not only slows the processing time considerably, but increasing the number of free parameters also increases the likelihood of obtaining a nonunique solution.

These problems were foreseen by *Kaper et al.* [1966]. Kaper et al. pointed out that mathematically, a discrete spectrum containing observational errors has, in general, no unique Gaussian deconvolution. The nonlinear least squares minimumization procedure used for Gaussian deconvolution (see the appendix) merely requires that a relative, not an absolute, minimum be obtained. It is quite possible to start from different initial estimates and arrive at different relative minima. In addition, while minimizing the RMS residual error provides an objective measurement for determining the "best" fit, it is in general always possible to reduce the RMS residual error by including additional Gaussians. Kaper et al. do however, suggest that if the signal to noise ratio is high and the components are well separated, there may in fact be a unique solution and requiring that the RMS residual error be of the order of the observational errors is sufficient.

It therefore appears that in its present form, the Gaussian model does not correspond with actual physical absorptions nor provide a feasible approach to extracting compositional information from unknown samples.

Modified Gaussian Model

If a mathematical model can be developed which can describe a single absorption band with only one distribution, many of the problems of the Gaussian model could be overcome. Such a model would decrease the number of distributions necessary to describe a spectrum, make the spectral deconvolution more stable, and be more physically realistic. Given the limitations of the Gaussian model for pyroxene electronic transition absorptions, it is appropriate to reexamine its numerous assumptions to determine whether such a model can be derived. One fundamental assumption of the Gaussian model is that energy is the random variable for all absorptions (charge transfer, electronic transition, molecular bending, stretching, and vibrational phenomena). However, for electronic transition absorptions, the energy of absorption is a function of the distortion and the average ligand-ion bond length of the crystal field site [*Burns*, 1970*a*]. In a crystal field site, the average bond length will vary due to random thermal vibrations and variations in the crystal site. Thus, the random variable for electronic transition absorption bands is not the energy of absorption but the average bond length.

With such an understanding, one can invoke the central limit theorem of statistics and consider the average bond lengths to be Gaussian distributed. Since the average bond length determines the energy of absorption, a Gaussian distribution of average bond lengths will map into a distribution of absorption energies. The crystal field theory description of electronic transition absorption [e.g., *Burns*, 1970*a*; *Marfunin*, 1979], suggests that the absorption energy (e) and the average bond length (r) are related by a power law:

$$e \propto r^{n} \tag{3}$$

Utilizing this power law relationship (equation (3)), a Gaussian distribution of average bond lengths can be mapped into a "modified" Gaussian distribution of absorption energies $m(x)$:

$$m(x) = s \cdot \exp\left\{ \frac{-(x^n-\mu^n)^2}{2\sigma^2} \right\} \tag{4}$$

Changing the exponent of $(x^n-\mu^n)$ corresponds to altering the symmetry of the distribution, *i.e.* the relative slope of the right and left wings.

The best value of the exponent n in equation (3) can be derived empirically. The 0.9-μm orthopyroxene absorption feature is chosen for this derivation since it is thought to be dominated by a single electronic transition band. Furthermore, in order to remove the complications of multiple scattering, a single-crystal transmission spectrum is used to derive the appropriate value of n. The RMS residual error of a single modified Gaussian distribution fit to the 0.9-μm absorption feature of the β–transmission spectrum of the Bamble enstatite, using several different values of n, is shown in Figure 9*a*. The transmission absorption band appears to be best fit using a modified Gaussian distribution with $n \approx -1.0$.

A similar test for the 0.9-μm absorption feature in reflectance spectrum of the Websterite enstatite is shown in Figure 9*b*. As with the transmission absorption feature, $n \approx -1.0$ results in the smallest RMS residual error. A comparison of the fits of various distribution models to the 0.9-μm reflectance absorption band is shown in Figure 9*c*. The Gaussian model ($n = 1.0$) produces an unacceptable fit, but a progressive improvement occurs (e.g., $n = -0.2$) until the best fit is achieved ($n = -1.0$).

Using single modified Gaussian distributions of the form

$$m(x) = s \cdot \exp\left\{ \frac{-(x^{-1}-\mu^{-1})^2}{2\sigma^2} \right\} \tag{5}$$

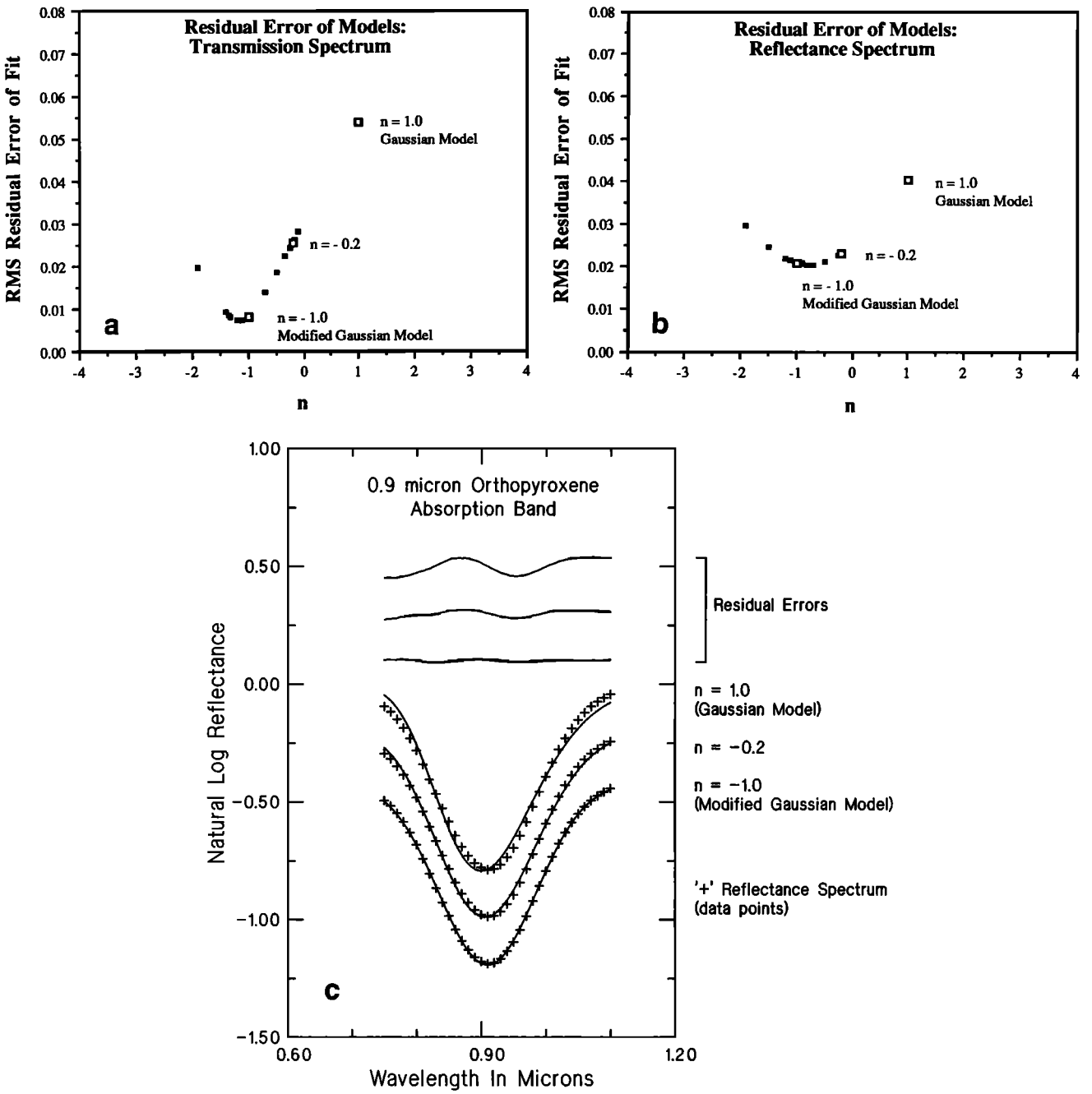

Fig. 9. The residual error between the 0.9-μm orthopyroxene absorption feature models using different values of n. (*a*) The β-transmission spectrum, (*b*) the 45-75 μm particle size reflectance spectrum, and (*c*) the <45 μm particle size reflectance spectrum. In all cases $n \approx -1.0$ produces the optimum fit. While $n = -1.0$ does not produce the lowest RMS residual error in all cases, the difference between the RMS residual error of the model with $n = -1.0$ and the lowest RMS residual error is negligible.

produces extremely accurate fits to the 0.9-μm pyroxene absorption band in both transmission and reflectance spectra. Modified Gaussian distributions thus appear to be a more physically realistic model of electronic transition absorption bands.

On the basis of these results, it appears that the absorption energy (e) and the average bond length (r) are inversely related and that equation (3) should read

$$e \propto r^{-1} \tag{6}$$

It is interesting to note that this relationship has the same $1/r$ dependence as the Coulombic potential energy of the crystal field site.

Results of the Modified Gaussian Model

To test this new model further the multiple features in extended pyroxene transmission and reflectance spectra were fit using a version of the fitting routine which deconvolves each spectrum into modified Gaussian distributions (see the appendix). The fit of the complete β–transmission spectrum of the Bamble enstatite, obtained with the modified Gaussian

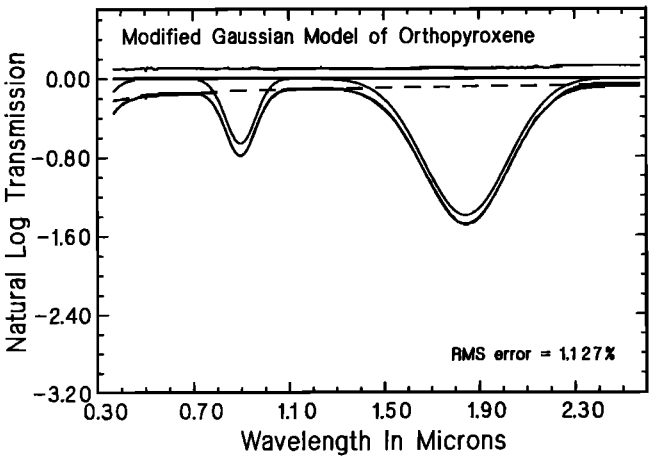

Fig. 10. The modified Gaussian model of the orthopyroxene β-transmission spectrum. Only single distributions are required for both of the absorption features near 1.0 and 2.0 μm.

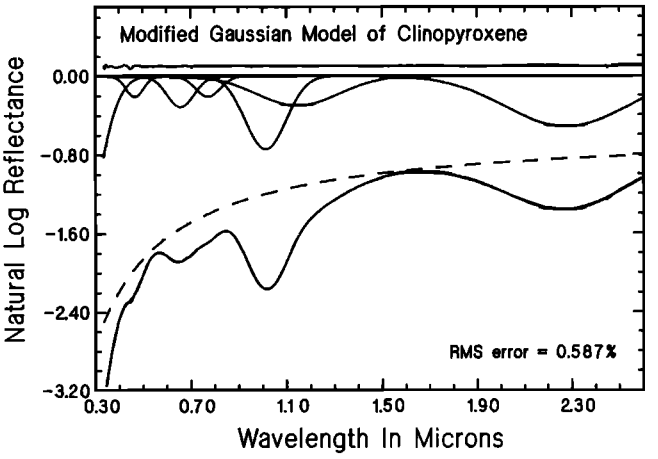

Fig. 12. The modified Gaussian model of the clinopyroxene reflectance spectrum (45-75 μm particles).

model is shown in Figure 10. This deconvolution requires only one modified Gaussian distribution for each of the absorption features near 1.0 and 2.0 μm. Nonetheless, the fit is quite remarkable. The modified Gaussian model of the orthopyroxene (Websterite) reflectance spectrum also requires only one distribution for each of the characteristic absorption features and also produces an excellent fit as shown in Figure 11. Similarly, the modified Gaussian model of the clinopyroxene reflectance spectrum is shown in Figure 12. Here again, the absorption feature near 2.0 μm is described by a single modified Gaussian distribution.

An essential test of the modified Gaussian model is whether it can correctly identify and characterize superimposed absorptions in mixture spectra. Unconstrained modified Gaussian analyses of the 75/25 and 25/75 Opx/Cpx mixture spectra are shown in Figure 13. Note that the distributions resulting from this unconstrained fit correspond directly to those found in the spectra of the orthopyroxene and clinopyroxene used to create these mixtures. As expected from the proportion of orthopyroxene in the mixture, the orthopyroxene features are significantly stronger than those of the clinopyroxene in the 75/25 Opx/Cpx mixture, while the clinopyroxene features dominate the 25/75 Opx/Cpx mixture.

The entire suite of 45-75 μm particle size orthopyroxene, clinopyroxene, and mass fraction mixtures is also fit using

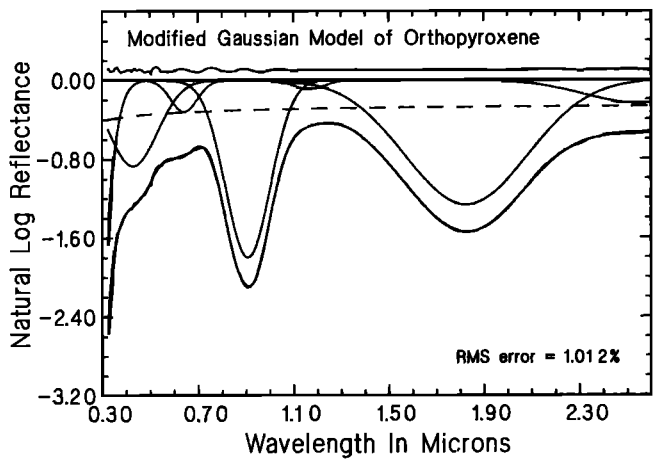

Fig. 11. The modified Gaussian model of the orthopyroxene reflectance spectrum (45-75 μm particles). Only single distributions are required for both of the absorption features near 1.0 and 2.0 μm.

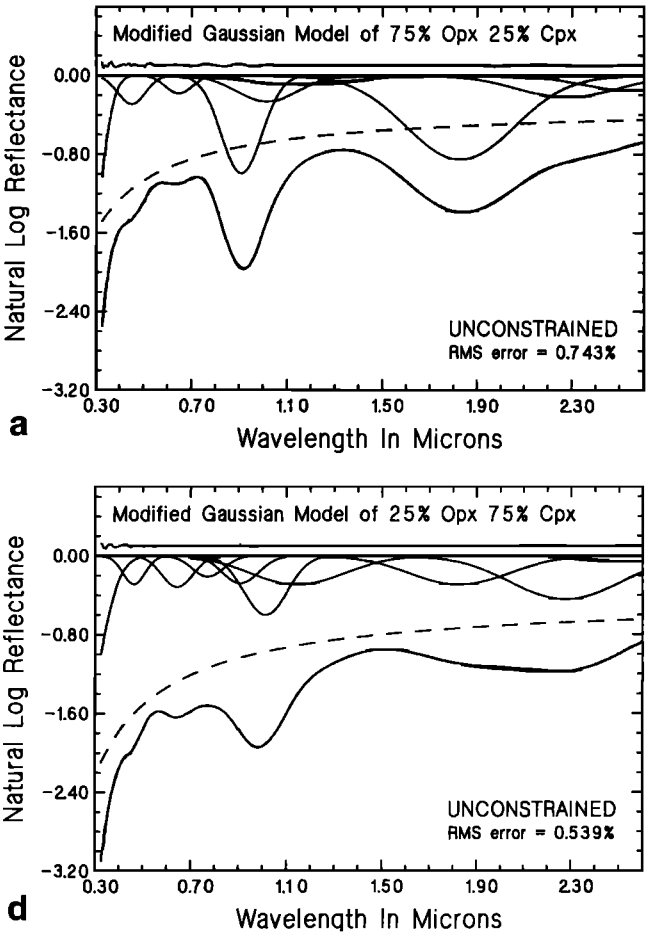

Fig. 13. (*a*) The Gaussian distribution model of the 75% orthopyroxene 25% clinopyroxene mixture reflectance spectrum (45-75 μm particles). (*b*) The modified Gaussian model of the 25% orthopyroxene 75% clinopyroxene mixture reflectance spectrum (45-75 μm particles). Unlike the Gaussian model, these fits are unconstrained, yet still reflect the proportion of clinopyroxene in each sample.

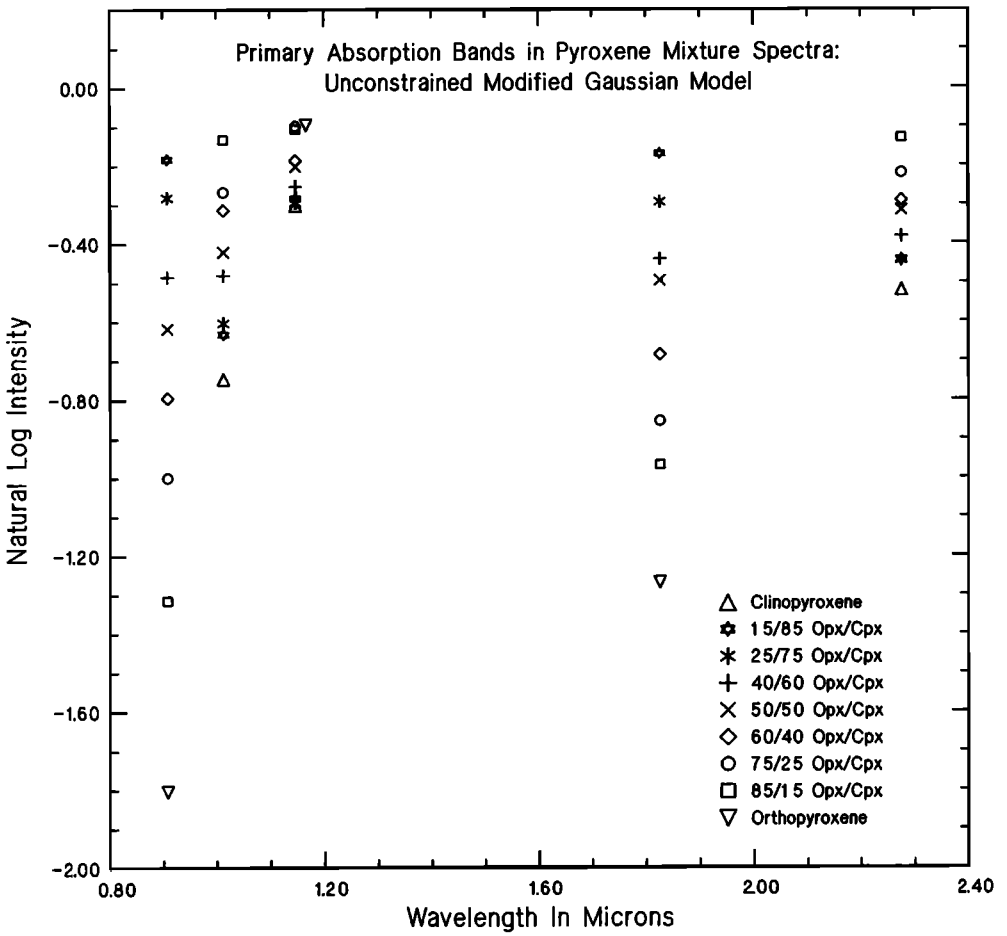

Fig. 14. The relative intensities of the modified Gaussian distributions that describe the primary absorption bands in the pyroxene and pyroxene mixture spectra (45-75 μm particles). Note the monotonic variation in band strength with proportion of clinopyroxene in the sample. Unlike the Gaussian model, the center of the distributions are not constrained to occur at the wavelengths determined for the orthopyroxene and clinopyroxene end-members.

unconstrained modified Gaussian distributions to determine if the new model reveals systematic and useful trends that correspond to the relative proportion of orthopyroxene and clinopyroxene found in each sample. Shown in Figure 14 are the strengths and band centers of the primary absorption bands derived for the entire suite of pyroxene mixture spectra. The band centers for each sample spectrum are determined independently yet occur at almost identical wavelengths for all mixture spectra. In addition, there is a monotonic variation in band strength which corresponds to the modal mineralogy of the sample. It should be noted that, unlike the Gaussian analysis, the modified Gaussian fits to the pyroxene mixture spectra are not constrained to have the bands centers occur at the same wavelengths as those found for the spectra of the pyroxene end-members. The fact that the bands centers of the mixture spectra are consistent with the bands centers of the two pyroxene end-member spectra lends further credence to the model.

On the basis of the success of the modified Gaussian model of electronic transition absorption bands in pyroxene spectra, a similar approach was applied to the more complex electronic transitions in olivine spectra. Given the overlap of absorptions in the olivine spectrum, it is not surprising that the olivine spectrum is also easily fit with modified Gaussian distributions (Figure 15). Yet, as can be seen by comparing the Gaussian and modified Gaussian models of the olivine reflectance spectrum (Figures 3 and 15), the two methods provide different assignments of absorption bands to the complex 1.0-μm feature. However, since the modified Gaussian model is shown to be more appropriate for pyroxene electronic transition absorption bands, the results from the modified Gaussian model are expected to provide a

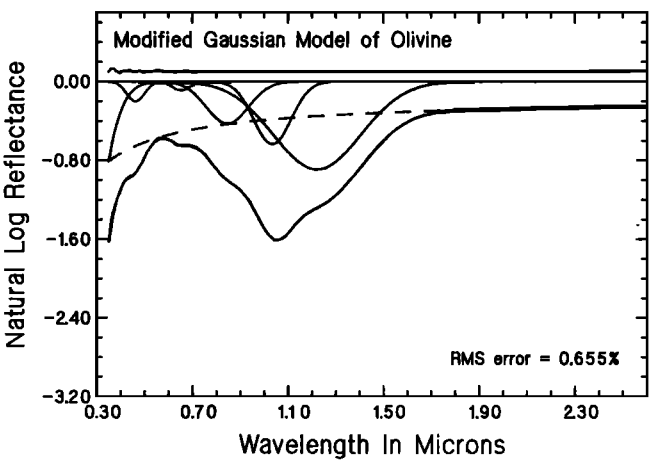

Fig. 15. The modified Gaussian model of the olivine reflectance spectrum (45-75 μm particles).

more appropriate characterization of the absorption bands in olivine spectra.

Conclusions

Deconvolving spectra into modified Gaussian distributions (equation (5)) is a physically realistic and practical model for characterizing the absorption features of both transmission and reflectance spectra. The ability of the modified Gaussian model to fit single electronic transition absorption bands with only one distribution represents a significant improvement over the Gaussian model. Modeling single absorption bands with single distributions is not only more physically realistic, but requiring fewer distributions decreases both the likelihood of nonunique solutions and the processing time.

Since absorption band assignments provide information about the nature of absorption sites, it is of the utmost importance that the correct deconvolution technique be used to describe absorptions in crystals. The ability of the modified Gaussian model to describe the absorption bands in both pyroxene and olivine spectra strongly suggests that it be the method of choice for analyzing electronic transition bands.

The success of the modified Gaussian model for electronic transition absorption bands is quite encouraging. It provides an objective and consistent method for deconvolving individual absorption bands from the spectra of pure samples and mixtures; as such, the analytical capacity of the modified Gaussian model has great potential. It can provide an invaluable tool for quantifying compositional trends from laboratory data and in identifying mineral constituents in remotely acquired spectra.

Although this study has shown that the Gaussian model is an inadequate description of electronic transition absorption bands, models for other absorption phenomena must be critically evaluated and, if necessary, alternate models must be derived. As is the case for the modified Gaussian model of electronic transition absorption bands, formulation of new models will undoubtedly focus on the determination of the random variable of absorption and how it relates to energy.

Appendix: Mathematics of the Gaussian Model

Mathematically, the Gaussian model of spectral deconvolution can be described by a nonlinear least squares analysis. The details of this procedure have been adapted for reflectance spectra based on the mathematics outlined by *Kaper et al.* [1966].

A spectrum, the percent reflectance measured at m discrete wavelengths, is first defined as a discrete function,

$$y(x_k), \quad k=1 \text{ to } m \tag{A1}$$

The spectrum is then approximated as a superposition of n Gaussian distributions with each individual Gaussian, $g(x_k)_i$, expressed in terms of its center (mean) μ_i, width (standard deviation) σ_i, and strength (amplitude) s_i:

$$g(x_k)_i = s_i \cdot \exp\left\{\frac{-(x_k-\mu_i)^2}{2\sigma_i^2}\right\} \tag{A2}$$

or

$$y(x_k) \approx G(x_k) = \sum_{i=1}^{n} g(x_k)_i \tag{A3}$$

Since each $g(x_k)_i$ has three parameters, μ_i, σ_i, s_i, and there are a total of n Gaussians, the spectrum is fully described by $3n$ parameters, or in vector form as a single $3n$ vector of parameters,

$$p \equiv (p_1, p_2, \ldots, p_{3n}) \tag{A4}$$

The accuracy of the approximation is determined by the residual difference between the actual spectrum and its model and is measured based on a sum of squares of the residuals, S, where

$$S \equiv \sum_{k=1}^{m} [y(x_k) - g(x_k)]^2 \tag{A5}$$

To produce a best fit to the spectrum, the sum of squares of the residuals (A5) must be of the same order of magnitude as the observational errors. This is determined by a least squares minimization of S (A5) with respect to the model parameters p (A4). This is accomplished by solving the normal equations

$$\nabla S = 0 \tag{A6a}$$

where

$$\nabla = \left(\frac{\delta}{\delta p_1}, \frac{\delta}{\delta p_2}, \ldots, \frac{\delta}{\delta p_{3n}}\right)$$

and

$$\frac{\delta}{\delta \mu_i} = \frac{g(x_k)_i\,(x_k-\mu_i)}{\sigma_i^2}$$

$$\frac{\delta}{\delta \sigma_i} = \frac{g(x_k)_i\,(x_k-\mu_i)^2}{\sigma_i^3}$$

$$\frac{\delta}{\delta s_i} = \frac{g(x_k)_i}{s_i}$$

or, from (A5),

$$\sum_{k=1}^{m} [y(x_k) - G(x_k)]\,\nabla G(x_k) = 0 \tag{A6b}$$

These normal equations (A6), form a set of $3n$ equations with $3n$ unknowns, p.

However, since $G = G(x_k)$ is itself nonlinear in p, the normal equations (A6) are also nonlinear and therefore cannot be solved directly. Instead, an iterative process is used to approximate p. Starting from an initial estimate, p_0, a sequence of vectors $\{p_j\}$ (j denoting the jth iteration) are calculated such that they converge to a vector p that satisfies (A6). Formally, $G = G(x_k)$ may be expanded into a Taylor series in Δp_j, where

$$\Delta p_j = p_{j+1} - p_j \tag{A7}$$

and

$$G_{j+1} = G_j + \nabla G_j \Delta p_j + \ldots \tag{A8}$$

Here, the higher order terms are disregarded as p_j approaches p. Under this expansion, the normal equations (A6b) can be rewritten as

$$\sum_{k=1}^{m} [y(x_k)-G_j(x_k) - \nabla G_j(x_k)\Delta p_j] \nabla G_j(x_k) = 0 \quad (A9a)$$

or

$$\sum_{k=1}^{m} [\nabla G_j(x_k)_j \Delta p_j] \nabla G_j(x_k) =$$

$$\sum_{k=1}^{m} [y(x_k) - G_j(x_k)_j] \nabla G_j(x_k) \quad (A9b)$$

Invoking matrix notation, the left-hand side of (A9*b*) can be written as

$$D_j \Delta p_j \quad (A10)$$

where

$$D_{nm} \equiv \frac{\delta G_j(x_k)}{\delta p_n} \cdot \frac{\delta G_j(x_k)}{\delta p_m}$$

The right-hand side of (A9*b*) can be expressed in terms of the sum of squares of the residuals (A5) as

$$- 1/2 \nabla S_j$$

where

$$\nabla S_j = - 2 \sum_{k=1}^{m} [y(x_k) - G_j(x_k)_j] \nabla G_j(x_k) \quad (A11)$$

Combining equations (A10) and (A11), equation (A9*b*) becomes

$$D_j \Delta p_j = - 1/2 \nabla S_j \quad (A12a)$$

or

$$\Delta p_j = D_j^{-1} (- 1/2 \nabla S_j) \quad (A12b)$$

Equation (A12*b*) is then used for the next iteration of p with

$$p_{j+1} = p_j + \Delta p_j \quad (A13)$$

and the entire process is repeated for $j = j+1$. Termination of the procedure takes place when there is a negligible improvement in the root mean square (RMS) error of the fit, where

$$\text{RMS} \equiv \sqrt{S/m} \quad (A14)$$

However, this procedure has not yet accounted for the fact that reflectance spectra, as indicated earlier, should be modeled in natural log reflectance and energy. In order to accomplish this we must transform equation (A3) into a discrete function in energy (x = energy) and log space so that

$$\ln y(x_k) \approx G(x_k) = \sum_{i=1}^{n} g(x_k)_i \quad (A15)$$

One final adjustment is necessary to account for the fact the Gaussians are superimposed onto a continuum. To include the effects of a continuum, the discrete energy spectrum should be modeled as

$$\ln y(x_k) \approx G(x_k) + C = \sum_{i=1}^{n} g(x_k)_i + C \quad (A16)$$

where $C = ax + b$, a is the slope, and b is the intercept of the continuum. The only effect this has on the mathematics outlined above is to add two additional model parameters, continuum slope and intercept to the problem. Doing so requires that

$$p \equiv (p_1, p_2, \cdots, p_{3n+2})$$

and

$$\nabla = \left(\frac{\delta}{\delta p_1}, \frac{\delta}{\delta p_2}, \cdots, \frac{\delta}{\delta p_{3n+2}} \right)$$

where

$$\frac{\delta}{\delta a} = x$$

and

$$\frac{\delta}{\delta b} = 1. \quad (A17)$$

Thus, applying this least squares procedure ((A1)-(A14)) using equations (A16) and (A17), a spectrum can be deconvolved into multiple Gaussian distributions which are superimposed onto a continuum.

The nonlinear least squares analysis for deconvolving spectra with modified Gaussian distributions (see modified gaussian model section) remains essentially as indicated above. However, the Gaussian distribution (A2) must be replaced with a modified Gaussian distribution of the form

$$m(x_k)_i = s_i \cdot \exp \left\{ \frac{-(x_k^{-1}-\mu_i^{-1})^2}{2\sigma_i^2} \right\} \quad (A18)$$

In addition, the partial derivatives (A6*a*) must be redefined as

$$\frac{\delta}{\delta \mu_i} = \frac{m(x_k)_i \ (x_k^{-1}-\mu_i^{-1}) \ \mu_i^{-2}}{\sigma_i^2}$$

$$\frac{\delta}{\delta \sigma_i} = \frac{m(x_k)_i \ (x_k^{-1}\mu_i^{-1})^2}{\sigma_i^3}$$

$$\frac{\delta}{\delta s_i} = \frac{m(x_k)_i}{s_i} \quad (A19)$$

Acknowledgments. We wish to thank G. Rossman for generously providing pyroxene transmission spectra Detailed and thoughtful reviews by P. Helfenstein and J. Mustard led to significant improvements in this manuscript. The microprobe facility at Brown University is supported by funds from the Keck Foundation and is operated by J. Devine. All reflectance spectra were obtained using RELAB, a multiuser facility supported by NASA grant NAGW-748. The financial support for this research, NASA grant NAGW-28, is greatly appreciated.

REFERENCES

Adams, J. B., Visible and near-infrared diffuse reflectance spectra of pyroxenes as applied to remote sensing of solid objects in the solar system, *J. Geophys. Res.*, *79*, 4829-4836, 1974.

Adams, J. B., Interpretation of visible and near-infrared diffuse reflectance spectra of pyroxenes and other rock forming minerals, in *Infrared and Raman Spectroscopy of Lunar and Terrestrial Materials*, edited by C. Karr, pp. 91-116, Academic, San Diego, Calif., 1975.

Burns, R. G., *Mineralogical Applications to Crystal Field Theory*, 224 pp., Cambridge University Press, New York, 1970*a*.

Burns, R. G., Crystal field spectra and evidence of cation ordering in olivine minerals, *Am. Mineral.*, *55*, 1608-1632, 1970*b*.

Clark, R. N., Water frost and ice: The near-infrared spectral reflectance 0.65-2.5 μm, *J. Geophys. Res.*, *86*, 3087-3096, 1981.

Clark, R. N., Deconvolution of reflectance spectra of mineral mixtures into component abundance and grain size (abstract), *EOS Trans. AGU*, *68*, 464, 1987.

Clark, R. N., and T. L. Roush, Reflectance spectroscopy: Quantitative analysis techniques for remote sensing applications, *J. Geophys. Res.*, *89*, 6329-6240, 1984.

Cloutis, E. A., M. J. Gaffey, T. L. Jackowski, and R. L. Reed, Calibrations of phase abundance, composition, and particle size distributions for olivine-orthopyroxene mixtures from reflectance spectra, *J. Geophys. Res.*, *91*, pp. 11,641-11,653, 1986.

Farr, T. G., B. A. Bates, R. L. Ralph, and J. B. Adams, Effects of overlapping optical absorption bands of pyroxene and glass on the reflectance spectra of lunar soils, *Proc. Lunar Planet. Sci. Conf., 11th*, 719-729, 1980.

Gaffey, M. J., Spectral reflectance characteristics of the meteorite classes, *J. Geophys. Res.*, *81*, 905-920, 1976.

Gaffey, S. J., Spectral reflectance of carbonate minerals in the visible and near-infrared (0.35-2.55 microns): Calcite, aragonite, and dolomite, *Am. Mineral.*, *71*, 151-162, 1986.

Hapke, B., Bidirectional reflectance spectroscopy, 1., Theory, *J. Geophys. Res.*, *86*, 3039-3054, 1981.

Hazen, R. M., P. M. Bell, and H. K. Mao, Effects of compositional variation on absorption spectra of lunar pyroxenes, *Proc. Lunar Planet. Sci. Con., 9th*, 2919-2934, 1978.

Huguenin, R. L., and J. L. Jones, Intelligent information extraction from reflectance spectra: Absorption band positions, *J. Geophys. Res.*, *91*, 9585-9598, 1986.

Hunt, G. R., and J. W. Salisbury, Visible and near-infrared spectra of minerals and rocks, I, *Mod. Geol.*, *1*, 283-300, 1970.

Johnson, P.E., M. O. Smith, S. Taylor-George, and J. B. Adams, A semi-empirical method for analysis of the reflectance of binary mineral mixtures, *J. Geophys. Res.*, *88*, 3557-3561, 1983.

Kaper, H. G., D. W. Smits, U. Schwarz, K. Takakubo, and H. Van Woerden, Computer analysis of observed distributions into gaussian components, *Bull. Astron. Inst. Neth.*, *18*, 465-487, 1966.

Körtum, G., *Reflectance Spectroscopy*, 336 pp., Springer-Verlag, New York, 1969.

Marfunin, A. S., *Physics of Minerals and Inorganic Materials*, 340 pp., Springer-Verlag, New York, 1979.

McCord, T. B., R. N. Clark, B. R. Hawke, L. A. McFadden, P. D. Owensby, C. M. Pieters, and J. B. Adams, Moon: Near-infrared spectral reflectance: A first good look, *J. Geophys. Res.*, *86*, 10,833-10,892, 1981.

McCord, T. B., et al. (Ed.), Reflectance spectroscopy in planetary science: Reviews and strategy for the future, *NASA Spec. Publ., SP-493*, 40 pp., 1988.

Mustard, J. F., and C. M. Pieters, Abundance and distribution of ultramafic microbreccia in Moses Rock Dike: Quantitative application of mapping spectroscopy, *J. Geophys. Res.*, *92*, 10,376-10,390, 1987.

Mustard, J. F., and C. M. Pieters, Photometric phase functions of common geologic minerals and applications to quantitative analysis of mineral mixture reflectance spectra, *J. Geophys. Res.*, *94*, 13,619-13,634, 1989.

Nelson, M. L., and R. N. Clark, Application of radiative transfer theory to the spectra of mineral mixtures (abstract), *Lunar Planet. Sci. Con., 19th* , 846-847, 1988.

Pieters, C. M., Mare basalt types on the front side of the Moon: A summary of spectral reflectance data, *Proc. Lunar Planet. Sci. Conf., 9th.*, 2825-2849, 1978.

Pieters, C. M., Strength of mineral absorption features in the transmitted component of near-infrared reflected light: First results from RELAB, *J. Geophys.. Res.*, *88*, 9534-9544, 1983.

Rossman, G. R., Pyroxene spectroscopy, in vol. 7, *Rev. Mineral., Pyroxenes*, edited by C. Prewitt, pp. 93-115, Mineralogical Society of America, Washington, D. C., 1980.

Roush, T. L., and R. B. Singer, Gaussian analysis of temperature effects on the reflectance spectra of mafic minerals in the 1-μm region, *J. Geophys. Res.*, *91*, 10,301-10,308, 1986.

Singer, R. B., Near-infrared spectral reflectance of mineral mixtures: Systematic combinations of pyroxenes, olivine, and iron oxides, *J. Geophys. Res.*, *86*, 7967-7982, 1981.

Smith, G., and R. G. J. Strens, Intervalence-transfer absorption in some silicate, oxide and phosphate minerals, in *The Physics and Chemistry of Mineral and Rocks*, edited by R. G. J. Strens, 583-612, John Wiley, New York, 1976.

Sunshine, J. M., C. M. Pieters, and S. F. Pratt, Gaussian analysis of pyroxene reflectance spectra (abstract), *Lunar Planet. Sci. Conf., 19th* , 1151-1152, 1988.

Sunshine, J. M., C. M. Pieters, and S. F. Pratt, Mathematical deconvolution of mineral absorption bands (abstract), *Lunar Planet. Sci. Conf., 20th* , 1087-1088, 1989.

Wendlandt, W. W., and H. G. Hecht, *Reflectance Spectroscopy*, 298 pp., Wiley-Interscience, New York, 1966.

Yon, S. A., and C. M. Pieters, Interactions of light with rough dielectric surfaces: Spectral reflectance and polarimetric properties, *Proc. Lunar Planet. Sci. Conf., 18th.*, 581-592, 1988.

C. M. Pieters, S. F. Pratt, and J. M. Sunshine, Department of Geological Sciences, Brown University, Providence, RI 02912.

(Received April 20,1989;
revised October 10, 1989;
accepted December 5, 1989.)